



OPEN

Application of graphene oxide in *Agrobacterium*-mediated genetic transformation and construction of a novel DNA delivery system for watermelon

Yuanqian Qin, Shengqi Hua, Lili Zhu, Pinpin Nie, Caizhu Yang, Fangzhou Xu, Defeng Wu & Wei Dong

Graphene oxide (GO) is widely used in biotechnology. The purpose of this study was to improve the efficiency of genetic transformation by constructing a delivery system based on GO. First, GO was applied in the traditional genetic transformation scheme for watermelons. We used hydroponics and tissue culture methods to determine the optimal concentration of GO for watermelon plant growth, we then used this concentration of GO for watermelon genetic transformation and found that GO can inhibit the growth of *Agrobacterium tumefaciens* and promote the growth of explants. This discovery can simplify the replacement of various culture media after explant infection, improve the regeneration rate of transgenic plants, and reduce experimental costs. To improve the efficiency of genetic transformation, a polymer-functionalized graphene oxide nanoparticle (GO-PEG-PEI) nanodelivery system was constructed, and the results showed that GO-PEG-PEI can transfer pCambia1300-GFP plasmids into intact plant cells. We found that sheet-like GO-PEG-PEI can effectively load GFP and form small GO-PEG-PEI-GFP complexes, which can deliver pCambia1300-GFP plasmids into plant cells. This research provides a new technique for molecular breeding.

Keywords GO, Watermelon plants, Genetic transformation, Growth promotion, Delivery system

Watermelon (*Citrullus lanatus*) is an important horticultural crop that is widely grown worldwide and is one of the most important tropical fruits in the world¹. Watermelon plant breeding is a key technology, due to the narrow genetic background of watermelon plants, it is difficult to cultivate innovative new varieties². By introducing genes, new crop varieties can be generated via molecular breeding, and this method is applicable to watermelons³. Among commonly used transgenic techniques, the pollen-tube pathway method is difficult to implement and has low transgenic efficiency, while the gene gun method is expensive and can damage cells⁴. Therefore, the genetic transformation of watermelon plants is mainly based on *Agrobacterium tumefaciens* (*A. tumefaciens*)-mediated methods⁵. The transgenic process faces problems related to *A. tumefaciens* contamination and difficulty in plant rooting. The traditional method involves increasing the concentration of antibiotics such as cefotaxim sodium salt (Cef) and Timentin to inhibit bacteria. However, raising the concentration of antibiotics to a certain level can inhibit plant growth⁶. However, in the genetic transformation of watermelon based on *A. tumefaciens*, plant regeneration is challenging, and the transformation efficiency is low; these problems urgently need to be addressed.

With the development of nanotechnology, nanomaterials have become widely used in medicine, agriculture, biomedicine, and other fields^{7,8}. Graphene oxide (GO) exhibits chemical properties that are more active than many of those of graphene⁹. GO is hydrophilic because it contains many oxygen-containing functional groups, such as hydroxyl and carboxyl groups¹⁰. In addition, GO has great potential for use in the delivery of biomolecules such as DNA or RNA, current research focuses mainly on animal studies. It can serve as a carrier to transport DNA or RNA, playing a synergistic role in inhibiting tumour cell proliferation¹¹. For example, the polyethylene glycol (PEG)- and polyethylene imine (PEI)- biofunctionalized graphene oxide (GO-PEG-PEI) complex can be used to transmit Stat3 siRNA and inhibit the growth of mouse malignant melanoma cells^{11–13}. However, there

School of Life Science, Henan University, Kaifeng 475004, Henan, People's Republic of China. ✉email: dongw@vip.henu.edu.cn

is still little research on the use of GO as a delivery system in plants, mainly due to the large size of untreated GO, which makes it difficult for it to penetrate plant cell walls. Research on GO applications in agriculture has revealed that it can affect seed germination and plant growth and development^{14–16}. GO has significant effects on the growth and development of olive, rape, *Arabidopsis*, tomato and other crops^{17–19}. Different concentrations of GO have different effects on plant growth and development, specific concentration of GO can promote the growth and development of plants, but high concentrations of graphene inhibit plant growth²⁰. Furthermore, GO has a strong inhibitory effect on bacteria and fungi^{21–23}.

This study focused on the following two aspects. First, the effects of GO on the growth and development of watermelon plants and the inhibition of *A. tumefaciens* were investigated. This is the first study to use GO to replace antibiotics that inhibit *A. tumefaciens* in a genetic transformation system. Second, GO has a large specific surface area, can be loaded with substances, and has the ability to aggregate and stabilize nucleic acids after polymerization with PEG and PEI. It can also retain the biological activity of coupled nucleic acid molecules. Instantaneous transformation of plants has been achieved by injecting spherical GO nanoparticle (GON) siRNA complexes into tobacco leaves²⁴. This study confirmed the effective genetic transformation of watermelon plants by GO-PEG-PEI using molecular biology methods such as GFP fluorescence and PCR, which is of great significance for improving the genetic transformation system of watermelon and promoting the development of watermelon molecular breeding.

Materials and methods

Materials

The “Ke xi” watermelon plants ($2n = 2x = 22$) were homozygotes inbred for eight generations at the experimental farm of the Henan University Genetics and Breeding Base in Kaifeng, China. GO was purchased from Guangdong Jiazhao New Materials Co., Ltd. in China (product name, TNGO; product number, 7782-42-5). The purchased GO powder had a thickness of 2 nm, lamellar diameter of 0.4 ~ 10 μm , tamping density of 600 g/L, starch content of 96%, carbon content of 46.9%, oxygen content of 55.8%, sulfur content of less than 3.6%, ash content of less than 2.8%, and particle size of less than 85%. The powder was prepared into a GO stock solution for plant treatment as follows. GO powder (0.1 g) was slowly added to 50 ml of ultrapure water. Ultrasonication was applied for five minutes per session, for a total of half an hour of ultrasound. Afterwards, the sample was sterilized under high pressure, and the resulting suspension had a pH of 5–6. Then, the hydroponic culture medium was prepared, an appropriate amount of the prepared GO solution was added to Murashige and Skoog (MS) liquid culture medium, and the mixture was stirred to form a uniformly dispersed liquid. The following components were used: sucrose and boric acid (Kermel Chemical Reagent Co., Ltd., Tianjin, China); agar, kanamycin sulfate (Kan) and Cef (Solarbio Technology Co., Ltd., Beijing, China); and 6-benzylamino purine (6BA) and kinetin (KT) (Biosharp Biotechnology Co., Ltd., Hefei, China).

Hydroponic GO–plant experiment and plant tissue culture conditions

First, a hydroponics experiment was conducted. Seedlings of Ke xi watermelon were grown in media supplemented with 0 mg/L, 75 mg/L, 150 mg/L or 300 mg/L MS liquid medium at 25 °C for 30 days. The same size culture bottle and the same intensity of light were used. Each concentration was repeated 7 times. The watermelon plants were all cultured in incubators at 28 °C for 16 h of light and 25 °C for 8 h of darkness with 70% humidity. Second, watermelon tissue culture experiments were conducted. Prepared callus tissue from watermelon plants infected with *A. tumefaciens* was clamped with tweezers and washed in sterile water until no adhered *A. tumefaciens* was visible on the surface. The watermelon plants were washed three times with sterile water and then transferred to a sterile conical flask containing culture medium. MS medium containing different concentrations of GO was used in this tissue culture experiment, after culture for a designated period, the level of *A. tumefaciens* contamination of the tissue-cultured seedlings was assessed, and the optimal GO concentration for plant tissue culture was determined. The hydroponics experiment simulated natural growth in an incubator to facilitate future practical application in agriculture. Tissue culture was carried out under sterile conditions, and *A. tumefaciens* growth was monitored during the transformation process.

Detection of phytoplankton in the MS liquid culture medium

Hydroponic production mainly cultivates crops in open environments, using nutrient solutions rich in various nutrients, which creates favorable conditions for the growth of phytoplankton such as algae, and can easily trigger explosive reproduction of phytoplankton in nutrient solutions. The massive reproduction of phytoplankton will bring a series of negative effects: on the one hand, it will consume nutrients in the nutrient solution, reduce dissolved oxygen, and release toxic metabolites, thereby reducing water quality; On the other hand, it also increases the risk of plants being attacked by pests and diseases²⁵. To investigate the effect of GO on the growth of phytoplankton in hydroponic culture medium, MS culture medium samples containing different concentrations of GO were collected for testing. One hundred microlitres of liquid was dropped onto a plankton counting board. Photos of different phytoplankton were obtained with a Ze Xi biological analysis instrument (MAS-HL, Zhejiang, China), and then the phytoplankton types and their quantities in each sample were calculated via automatic data analysis software.

Plant transformation

The binary vector pCAMBIA1301 with GFP reporter gene was constructed as previously described²⁶. The candidate genes were inserted between the *SalI* and *SpeI* sites in the vector with the primers 1301-F and 1301-F (Supplementary materials Table 2). The resulting recombinant vectors were inserted into *A. tumefaciens* strain GV3101 cells.

Ke xi watermelon explants were transformed according to a modified method^{26,27}. In particular, after surface treatment, seeds were sown in the dark for 2 days in 6% agar solid culture medium (Supplementary materials Table 3) and for 1 day under a 16-h/8-h light/dark photoperiod. *A. tumefaciens* strain GV3101 harbouring the binary vector was used for transformation. The transformed watermelon explants were placed on SAM coculture medium and incubated under dark conditions at 28 °C for three days. The cotyledon explants were cultivated in different shoot induction media (SIMs) for 4 weeks and transferred onto different shoot elongation media (SEMs) for 3 weeks. The SIMs included two types: the first type included MS, 1.0 mg/L 6BA, 30 mg/L Kan and 300 mg/L Cef; in the second type, cephalosporin was replaced with GO, and the components were MS, 1.0 mg/L 6BA, 30 mg/L Kan and 150 mg/L GO. The SEMs included two types: the first type included MS, 0.2 mg/L kinetin (KT), 30 mg/L Kan and 300 mg/L Cef; in the second type, cephalosporin was replaced with GO, and the components were MS, 0.2 mg/L KT, 30 mg/L Kan and 150 mg/L GO. Plantlets with well-developed roots were taken from the culture medium and placed in plastic cups containing vermiculite. The growth status of the explants was examined. After four weeks of growth in the SIMs, the number of adventitious buds in each group of explants was counted, with ten explants per type, and this process was repeated three times. After three weeks of growth in the SEMs, the number of adventitious roots in each group of explants was counted, with ten explants per type, which was repeated three times. At the same time, DNA was extracted from the leaves of each explant, and PCR validation was performed using the primers GFP-F and GFP-R (Supplementary materials Table 2) to determine the positive transformation efficiency under different treatments. The transgenic seedlings were observed under fluorescence observation (LUYOR-3415RG, China, Shanghai).

Preparation of GO-PEG-PEI-GFP nanomaterials

The nanomaterial preparation method was based on a previously described method, with slight modifications as follows¹¹. One hundred milligrams of GO was added to 100 mL of sterile water, and a uniform transparent colloidal solution was prepared via ultrasonication. Then, 25 mmol NaOH and 8 mmol monochloroacetate were added to the GO solution, which was sonicated for 2 h. Then, 0.4 mmol EDC and 0.4 mmol NHS were added to 0.5 mg/ml GO-COOH solution and sonicated for 1 h. PEI was added to the GO solution at a mass ratio of 1:80, stirred for 24 h and then dialyzed for three days in a 100 kDa dialysis bag. Then, 20 mg of PEG was added to 10 ml of 0.5 mg/ml GO-PEI solution and stirred overnight. The mixture was then dialyzed in a 100 kDa dialysis bag for three days. The pCAMBIA1300-GFP plasmid was mixed with GO-PEI-PEG at a mass ratio of 1:0.5 and incubated at room temperature for 30 min. The prepared nanomaterials were stored at low temperature until use.

Characterization of the nanomaterials

To characterize the GO material, particle size analysis, zeta potential analysis, and electron microscopy imaging were performed. A Zetasizer Nano ZS nanoparticle size potential analyser was used to measure the nanoparticle size and zeta potential of the dispersion. The analyser measures samples on the basis of the principle of electrophoretic light scattering, and an excitation wavelength of 633 nm was applied. The specific steps were as follows: the machine was preheated for 20 min, the Zetasizer software was opened on the computer, “dispersant dispersant, 25 °C, 120 s” was selected, the prepared sample dispersion was transferred to a colorimetric dish and a zeta potential sample cell, the sample cell was placed in the instrument for particle size and zeta potential measurement, and the dispersion stability of the product was determined on the basis of the measured values.

TEM was conducted using a Sevier HT7700 transmission electron microscope. The specific steps were as follows: a pipette was used to extract 20 µl of the nanomaterial suspension, which was dropped onto a carbon film copper mesh and incubated for 3–5 min, after which filter paper was used to remove excess liquid. 2% phosphotungstic acid was dropped onto the carbon-supported copper mesh and allowed to sit for 1–2 min. Filter paper was used to remove excess liquid, and the mixture was dried at room temperature. Images were obtained for analysis under a transmission electron microscope.

Effect of nanomaterials on pollen tube elongation

Mature pollen was dropped onto a slide with forceps, and pollen tubes were induced using pollen tube germination BM (Supplementary materials Table 3). After 30 min, 0, 12, 32, 64 or 93 mg/ml nanomaterial carrier was added, and then the growth of the pollen tubes was observed under a microscope (Nikon ECLIPSE Si, Japan) after 1 h and 2 h.

Construction of a delivery system based on GO-PEG-PEI

To improve the conversion efficiency of the pollen-tube pathway method, a GO-PEG-PEI-GFP delivery system was constructed. The pollen-tube pathway method involves injecting a DNA solution containing the target gene into the ovary after pollination and integrating it into the genome to complete the transformation²⁸. The first step involved self-pollination of homozygous watermelon. Two hours later, the GO-PEG-PEI-GFP nanomaterials were applied to the stigma of the female flowers of watermelon. After the infected watermelon was mature, the watermelon seeds were peeled out, the fluorescence was observed using a laser gun, and the DNA was extracted. The transgenic efficiency was detected using the primers GFP-F and GFP-R (Supplementary materials Table 2).

Results

GO affects the growth of watermelon plants

To verify the effect of GO on watermelon plants, hydroponic experiments were performed, and observations were conducted once a week. When the concentration of GO was 75 mg/L or 300 mg/L, GO treatment had a significant inhibitory effect on the growth of roots, and the average root lengths were 5 cm and 8 cm, respectively. However, when the concentration reached 150 mg/L, GO treatment significantly promoted the growth of watermelon roots, and the average root length was 11.3 cm, approximately 2.9 cm longer than that of the control.

The results showed that 150 mg/L GO promoted the growth of watermelon roots. The changes in the watermelon plants were similar to those in the roots. Treatment with 75 mg/L or 300 mg/L GO had a significant inhibitory effect on the growth of watermelon plants. When the concentration of GO was 150 mg/L, the watermelon plants were the longest at approximately 20 cm long, 1.7 cm longer than that in the control. Therefore, 150 mg/L GO significantly promoted the growth of watermelon plants. However, GO treatment had no significant effect on the growth of the aboveground stems of watermelon plants (Fig. 1).

GO affects the growth of *A. tumefaciens* and phytoplankton

To test the inhibitory effect of GO on *A. tumefaciens* carrying transgenic vectors, watermelon genetic transformation experiments were conducted. Figure 2A a, b, c, and d show images of MS solid culture medium supplemented with 300 mg/L Cef and 75 mg/L, 150 mg/L and 300 mg/L GO. Microscopic examination revealed that the culture media containing 75 mg/L GO and 300 mg/L Cef both contained *A. tumefaciens*. The addition of 150 mg/L and 300 mg/L GO to the culture medium significantly inhibited *A. tumefaciens* (Fig. 2B, a). To assess the natural growth of phytoplankton in MS liquid medium with GO, a biological analyser was used to detect the species and quantity of phytoplankton. The results showed that the number of algae significantly decreased in the culture medium supplemented with GO (Fig. 2B, b). *Chlorella vulgaris* (*C. vulgaris*) and *Chlamydomonas* were the most abundant green algae. The number of these two algae in the culture medium containing GO was relatively small, and GO effectively inhibited the growth and reproduction of these algae.

GO promotes the regeneration of explants

To determine the impact of GO on explants in genetic transformation, the optimal GO concentration was selected for genetic transformation experiments. As shown in the example figure, watermelons are genetically transformed using different media (Fig. 3A, B). After three weeks of growth in elongation media, the seedlings in the GO treatment began to take root. By counting the number of adventitious buds and roots of plants in different culture media, it was shown that 150 mg/L GO significantly promoted the growth of adventitious buds and roots of the explants (Fig. 3C, D). Observe the fluorescence status of plants grown in the culture medium after two and three weeks of growth. PCR revealed that the positive conversion rate under normal culture conditions was 22.7%, whereas under GO culture conditions, the positive conversion rate was 25.9% (Fig. 3E).

Effect of GO-PEG-PEI-GFP on pollen tubes

To determine the effect of GO-PEG-PEI-GFP on pollen tubes, the toxicity of different concentrations of GO-PEG-PEI-GFP to pollen tubes was tested. After 30 min in pollen tube induction medium, the pollen tubes developed well (Fig. 4A, a–e). Subsequently, different concentrations of nanomaterials were added; after 1 h, the higher the concentration of nanomaterial was, the more wrinkled the pollen grains became, but the effect on the pollen tubes was not significant (Fig. 4A, f–j). After 2 h, there was still no significant effect on the pollen tubes (Fig. 4A, k–o). Calculation of the pollen germination rate at different concentrations revealed that different concentrations of GO-PEG-PEI-GFP had no significant effect on the pollen tube germination rate (Fig. 4B, a). Calculation of the length of pollen tubes at different concentrations and times indicated that after 2 h, GO-PEG-PEI-GFP at concentrations of 32, 64, and 93 mg/ml had a significant effect on the length of pollen tubes (Fig. 4B, b). The pollen toxicity experiment proved that the most suitable concentration of GO-PEG-PEI-GFP was 12 mg/ml.

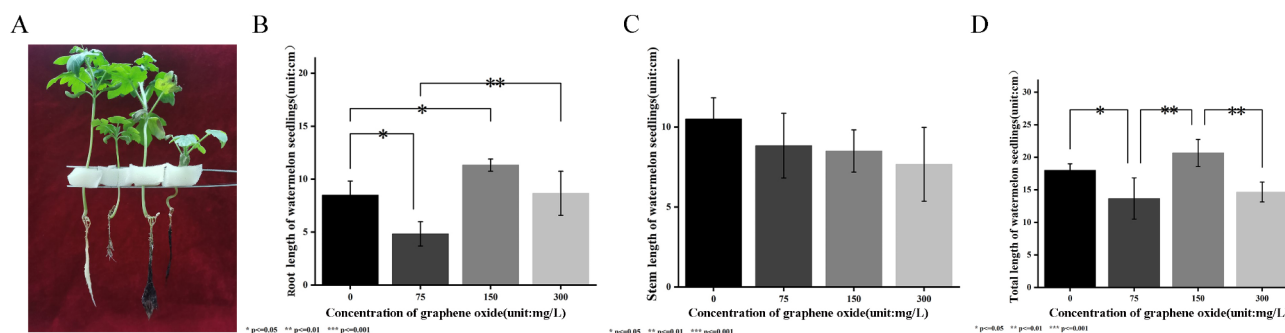


Fig. 1. Hydroponic growth chart. (A) Comparison of the main roots of watermelon plants after two weeks of growth. (B) Effects of GO on the main root; 0, 75, 150, and 300 refer to different concentrations of GO. The error lines on the columns represent the standard deviation, and the “*” annotations on the chart represent significant differences between different treatments. (C) Effects of GO on stem length; 0, 75, 150, and 300 refer to different concentrations of GO. The error lines on the columns represent the standard deviation, and the “*” annotations on the chart represent significant differences between different treatments. (D) Effect of GO on overall length; 0, 75, 150, and 300 refer to different concentrations of GO. The error lines on the columns represent the standard deviation, and the “*” annotations on the chart represent significant differences between different treatments. (* p < 0.05 ** p < 0.01 *** p < 0.001).

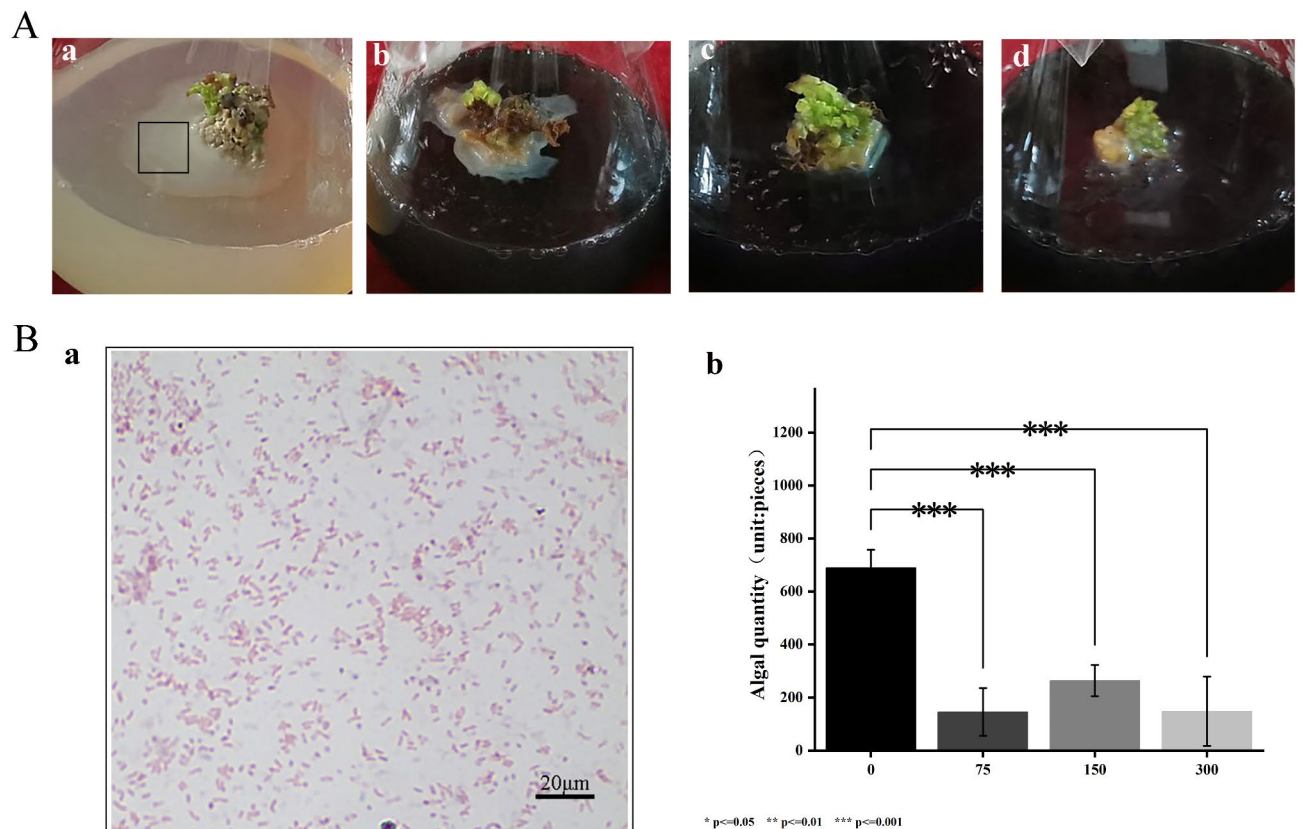


Fig. 2. Hydroponic culture medium and its microscopic changes. (A) a, b, c, d show images of MS solid culture medium supplemented with Cef and 75 mg/L, 150 mg/L and 300 mg/L GO. (B) (a), Results of Gram staining of *A. tumefaciens* picked from the culture medium. (b), Statistics on the number of algae in culture media with different concentrations of GO added, with different letters on the graph indicating significant differences between different treatments (* $p < 0.05$ ** $p < 0.01$ *** $p < 0.001$).

The nanodelivery system promotes genetic transformation efficiency

In accordance with the design process, we prepared the nanomaterial GO-PEG-PEI-GFP and delivered the pCambia1300-GFP plasmid into watermelon (Fig. 5A). The pCambia1300-GFP plasmid was loaded onto the prepared GO-PEG-PEI by electrostatic adsorption to form a GO-PEG-PEI-GFP nanomaterial complex. pCambia1300-GFP and GO-PEG-PEI were mixed at a mass ratio of 1:0.5 for 30 min at room temperature. The results of gel electrophoresis showed that pCambia1300-GFP was fully loaded at this time (Fig. 5B, a). Zeta potential analysis showed that after GO was modified with PEG and PEI, the potential increased from -11.5 mV to 31.5 mV. After loading with the pCambia1300-GFP plasmid, the potential did not differ from that of GO-PEG-PEI alone, indicating that the pCambia1300-GFP plasmid had no significant effect on the carrying capacity of GO-PEG-PEI (Fig. 5B, b). Interestingly, after loading the pCambia1300-GFP plasmid, the particle size of the GO-PEG-PEI-GFP complex significantly decreased and was significantly smaller than that of GO-PEG-PEI (Fig. 5B, c). The nanomaterials were ultrasonically dispersed to form a uniform yellow transparent liquid, and electron microscopy revealed an irregular layered structure (Fig. 5C, a). There was no difference between the electron microscopy images of GO-PEG-PEI and GO-PEG (Fig. 5C, b), indicating that the nanomaterials are relatively stable. After the addition of the pCambia1300-GFP plasmid, the plasmid was enveloped by GO-PEG-PEI (Fig. 5C, c). By using the pollen tube channel method, GO-PEG-PEI-GFP vectors were transferred into watermelons, and green fluorescence was observed in watermelons grown for 1 day, 10 days, or 30 days (Fig. 5D, a, b, c). During the experiment, we obtained three watermelons. We randomly extracted DNA from four batches of watermelon seeds, each containing 30 seeds, and analysed them via PCR. The number of positive seeds in each batch was 27, 24, 13, and 8. After calculating the positivity rate of each batch, the average was calculated as the output value. The conversion efficiency was calculated to be 59.33%.

Discussion

GO is a type of carbon nanomaterial and is biocompatible. Through hydroponic experiments, the following two conclusions were reached. First, GO significantly promotes watermelon plant growth, providing a foundation for the application of nanomaterials in watermelon plant cultivation. Research has shown that low or high concentrations of GO may inhibit plant growth due to toxic effects or oxidative stress, while the promoting effect of GO on plants is related to increased antioxidant enzyme activity and indole-3-acetic acid levels²⁹. This study revealed that at lower concentrations (75 mg/mL) and higher concentrations (150 mg/mL), GO inhibited

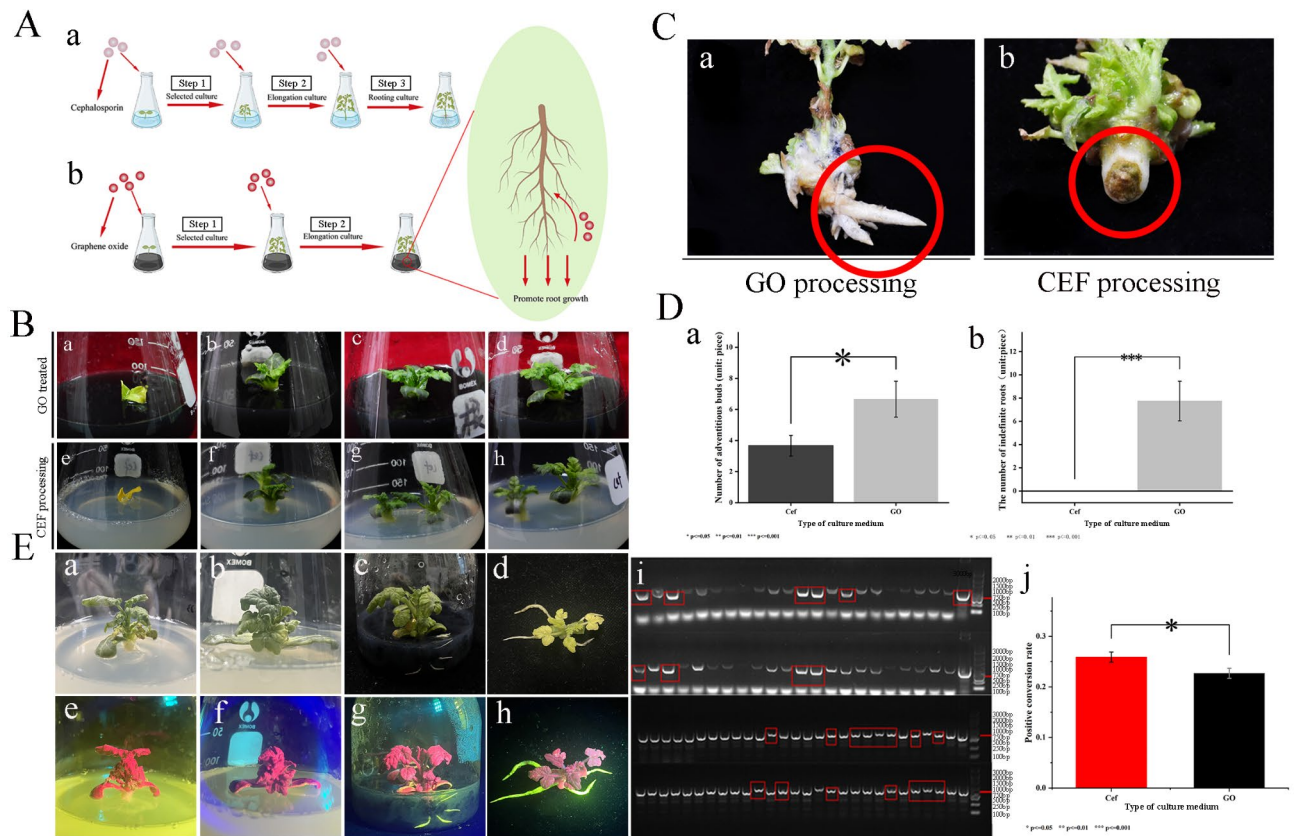


Fig. 3. Comparison of genetic transformation. **(A)** Experimental schematic of genetic transformation using GO: (a) normal genetic transformation process of watermelon; (b) genetic transformation process of watermelon with added GO; **(B)** comparison of genetic transformation at different stages with the addition of GO and cephalosporin; **(C)** comparison of root growth after three weeks of growth in elongation medium: (a) explants cultured with GO, (b) explants cultured through normal genetic transformation; **(D)** statistics on the number of adventitious buds and roots produced by explants grown in different media (* $p < 0.05$ ** $p < 0.01$ *** $p < 0.001$); **(E)** (a), (c) growth in normal elongation medium after two weeks and fluorescence results, (b), (f) growth in normal elongation medium after two weeks and fluorescence results; (c), (g) growth in graphene oxide elongation medium after two weeks and fluorescence results, (h) growth in graphene oxide elongation medium after three weeks and fluorescence results, (i) PCR results for transgenic seedlings; (j) positive conversion rate of explants in different culture media (* $p < 0.05$ ** $p < 0.01$ *** $p < 0.001$).

plant growth. Moreover, there is an optimal concentration for the promoting effect of GO on watermelon plants, which is similar to the phenomenon in other crops. In a previous study, GO inhibited the growth of cabbage, tomato, amaranth, and lettuce seedlings, and the degree of inhibition was positively correlated with the GO concentration³⁰. However, GO treatment promoted the growth of hydroponic buckwheat seedlings. With increasing GO particle size or concentration, the overall growth indicators of buckwheat seedlings showed a trend of first increasing and then decreasing³¹. Second, GO can significantly impact the number and types of phytoplankton in liquid media, providing a foundation for the hydroponic cultivation of nanomaterials in nonsterile environments. GO has a significant inhibitory effect on *C. vulgaris* and *Chlamydomonas*, but a certain concentration of GO can increase the protein, total lipid, and carbohydrate contents in algae cells, providing energy for the algae to protect themselves and adapt to stress³². GO, reduced graphene oxide (RGO) and graphene, which can exist in *C. vulgaris* in their original form or be adsorbed by EPS, hinder the growth and photosynthetic activity of algae at relevant concentrations³². Interestingly, these previous results were consistent with the results for watermelon plant seedlings in this study. GO at low and high concentrations significantly inhibited the growth of algae in MS liquid culture medium. Graphene photocatalysis can significantly reduce species richness in the treatment area and is expected to become a new green technology for reducing harmful algae in water³⁴. We are conducting molecular mechanism research to provide support for comprehensive application of GO in biology.

GO can replace antibiotics and promote plant regeneration. First, GO can inhibit genetically modified *A. tumefaciens*, suggesting that it could be applied as a substitute for antibiotics. GO inhibits the growth of gram-negative bacteria, mainly *E. coli* and *S. aureus*. RGO nanomaterials have been proven to have toxic effects on *E. coli*, in studies, *E. coli* died upon contact with nanomaterials, mainly due to the adhesion of nanomaterials to the cell surface, leading to the rupture of the cell membrane structure³⁵. When GO acts on cell suspensions, the antibacterial mechanism is mainly cell capture, and large GO has good antibacterial activity³⁶. The sharp nano-

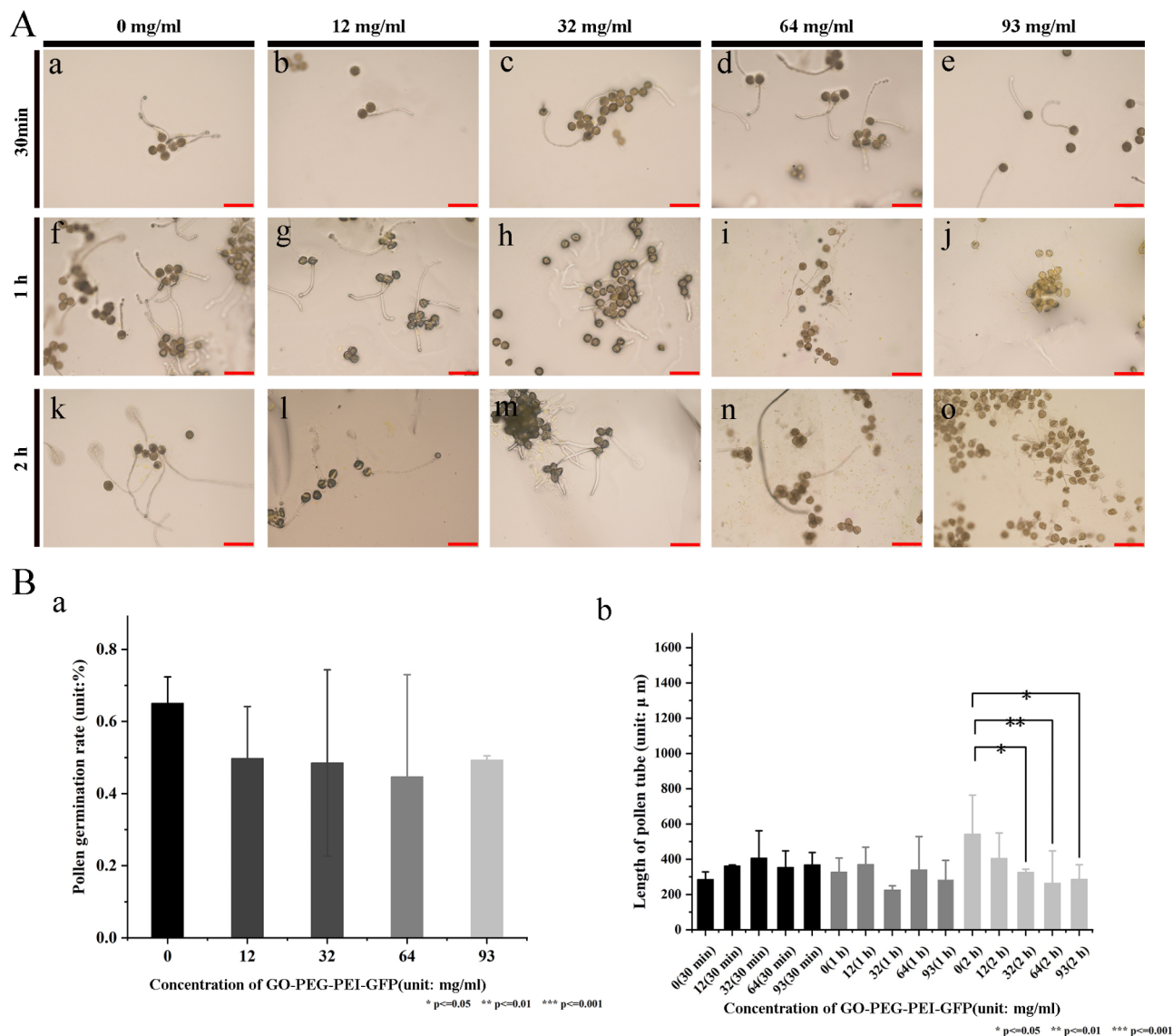


Fig. 4. Analysis of nanomaterial toxicity. (A) (a) (f), (k) Pollen cultured in medium without added GO; (b), (g), (l) pollen cultured in medium with 12 mg/ml GO added; (c), (h), (m) pollen cultured in medium with 32 mg/ml GO added; (d), (i), (n) pollen cultured in medium with 64 mg/ml GO added; (e), (j), (o) pollen cultured in medium with 93 mg/ml GO added (bar = 200 μ m). (B) Pollen tube germination rate and pollen tube length: (a) germination rate at different concentrations; (b) pollen tube length at different times and concentrations (* $p < 0.05$ ** $p < 0.01$ *** $p < 0.001$).

edges in GO can cut bacterial cells into fragments³⁷. GO derivatives are expected to be used as supplements to clinically relevant antibiotics³⁸. Forrest Nichols et al. sought to enhance the bactericidal effect by synthesizing nanocomposites to replace antibiotics³⁹. Second, GO can promote the growth of adventitious buds in watermelon plants, providing a foundation for the application of nanomaterials in watermelon plant molecular breeding. Consistent with previous research, GO had a positive effect on the performance of plantain callus histiocytes at a specific concentration⁴⁰. Third, GO can promote the rooting of genetically modified seedlings, further supporting the application of nanomaterials in watermelon plant molecular breeding. GO can not only promote the elongation of adventitious roots in cotinus coggygia tissue cultured seedlings, but also promote the growth of rice roots^{6,41,42}. In addition, various indicators of raspberry tissue-cultured seedlings showed a trend of first increasing and then decreasing with increasing GO concentration⁴³. These findings indicate that GO has the advantages of low price, antibacterial effects and the ability to promote the growth of watermelon transgenic plants.

In this study, considering the unique properties of pollen tubes, we constructed the GO-PEG-PEI delivery system to achieve efficient genetic transformation. First, a GO-PEG-PEI-GFP nanocomposite was constructed using the pCAMBIA1300-GFP plasmid and GO-PEG-PEI. The feasibility of the GO-PEG-PEI delivery system was validated by transferring the pCAMBIA1300-GFP plasmid into watermelon. Many studies have used GO-

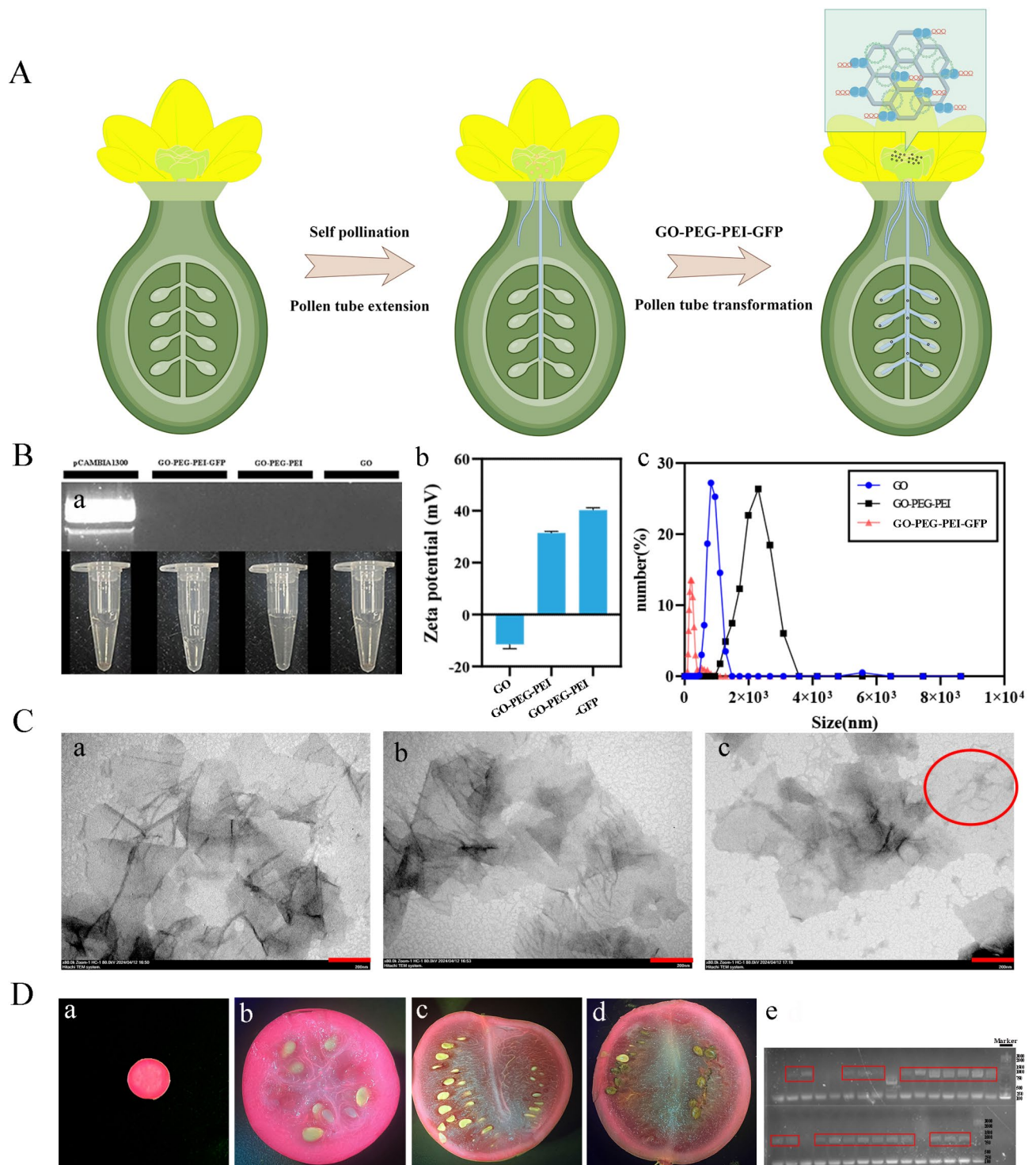


Fig. 5. The GO-PEG-PEI nanodelivery system promotes genetic transformation efficiency. **(A)** Diagram of the GO-PEG-PEI-GFP preparation process; **(B)** testing and characterization of nanomaterials; **(a)** electrophoresis images of the pCAMBIA1300-GFP plasmid, GO-PEG-PEI-GFP, GO-PEG-PEI, and GO; **(b)** zeta potential analysis results for GO, GO-PEG-PEI, and GO-PEG-PEI-GFP; **(c)** particle size analysis results for GO, GO-PEG-PEI, and GO-PEG-GFP; **(C)** electron microscopy images corresponding to the GO-PEG-PEI-GFP preparation process: **(a)** electron microscopy image of GO; **(b)** electron microscopy image of GO-PEG-PEI; **(c)** electron microscopy image of GO-PEG-PEI-GFP; **(b = 200 μ m)**; **(D)** fluorescence images of transgenic watermelons at 1 day, 10 days, and 30 days, as well as an electrophoresis image used to assess transgenic efficiency: **(a)** cross section of watermelon grown for one days after genetic transformation; **(b)** cross section of watermelon grown for ten days after genetic transformation; **(c)** cross section of watermelon grown for 30 days after genetic transformation; **(d)** cross section of watermelon grown for 30 days under normal conditions (negative control); **(e)** Transgenic efficiency.

PEG-PEI to deliver genes to animal cells. For example, GO-PEG-PEI loading and delivery of miR-29b promoted BMSC osteogenic differentiation and bone regeneration⁴⁴. The extracellular vesicles of herbs can successfully bind to chitosan, PEG and GO and then bind to oestrogen receptor α -targeted siRNA for delivery to breast cancer MCF7 cells⁴⁵. The main reason for the above results is that animal cells do not have cell walls, which might otherwise obstruct the delivery of nanomaterials. Second, this research bypasses instantaneous plant transformation and realizes stable transformation. After pollination, DNA can enter the embryo sac along the pollen tube channel and integrate into the genome to achieve stable transformation. *Arabidopsis* species have a cysteine-rich peptide (AtLURE1 peptide) that can guide pollen tubes into the ovule pore, but only pollen tubes of the same species can be effectively attracted at appropriate protein concentrations⁴⁶. GO can efficiently and quickly transport plasmids into watermelon via the pollen tube channel method. GONs can transfer siRNA into cells to achieve transient gene silencing²⁴. In addition, the genetic transformation efficiency of the pollen tube pathway method is only 2.5%, and that of *Agrobacterium* is approximately 6.7%^{47,48}, compared to the previous two methods, in this study method not only improves the efficiency of genetic transformation but also avoids the tedious steps required in aseptic operations. Thirdly, PEG modified PEG-PEI can shield the high density of positive charges in PEI, thereby reducing cytotoxicity and improving the transfection efficiency of GO-PEG-PEI on specific cells, which meets the requirements of genetic transformation⁴⁹. And the appropriate concentration of nanomaterials will not affect pollen development or fruit growth. Research has shown that using magnetic nanoparticles loaded with exogenous DNA to transfer into pollen through the pores of plant cell membranes under the action of a magnetic field does not cause damage to pollen, and exogenous DNA can be successfully internalized in pollen grains and pollen tubes⁵⁰. 100-fold dilution of chitosan quaternary ammonium salt dsRNA nanoparticles (HACC dsRNA NPs) has no negative effect on pollen viability, and pollen can serve as a pathway for dsRNA to enter seeds⁵¹. In vivo assays have demonstrated that GO-PEG-PEI-CpG and GO-PEG-PEI/siRNA complexes have low cytotoxicity and excellent therapeutic efficacy^{52,53}. This study revealed that the GO-PEG-PEI nanocomplex has good biocompatibility, plasmid loading capacity, and transfection efficiency in watermelon plants.

In summary, this study simplifies the steps of genetic transformation, reduces the use of antibiotics, and reduces experimental costs, making it an effective innovation in genetic transformation experiments. In addition, a delivery system was established in watermelon plants, achieving rapid genetic transformation. The emergence of nanobiotechnology has provided unprecedented opportunities to accelerate molecular breeding.

Data availability

All data generated or analysed during this study are included in this published article [and its supplementary information files].

Received: 9 September 2024; Accepted: 4 February 2025

Published online: 14 February 2025

References

- Zheng, Y. P. Global characteristics and trends of researches on watermelon: based on bibliometric and visualized analysis. *Heliyon* **10**, e26824 (2024).
- Sarria, E. Global challenges for the future of watermelon plant breeding. *Acta Hort.* **2017**, 5–8 (2017).
- Guo, S. Resequencing of 414 cultivated and wild watermelon accessions identifies selection for fruit quality traits. *Nat. Genet.* **51**, 89 (2019).
- Chun, R. Genetic transformation in watermelon by using gene-gun. *J. Hunan Agricultural Univ.* **26**, 74 (2000).
- Vasudevan, V., Sathish, D., Ajithan, C., Sathish, S. & Manickavasagam, M. Efficient agrobacterium-mediated in planta genetic transformation of watermelon [*Citrullus lanatus* Thunb]. *Plant. Biotechnol. Rep.* **15**, 447–457 (2021).
- Chen, T. et al. Effect of graphene oxide on adventitious root formation in tissue cultured seedlings of *Cotinus coggygia* in the United States. *Inner Mongolia Forestry Invest. Des.* **42**, 97–100 (2019).
- Cao, T. et al. Effect of Graphite oxide on wheat seed germination and seedling growth under salt stress. *J. Shanxi Agric. Univ.* **42**, 84–92 (2022).
- Rattana et al. Preparation and characterization of graphene oxide nanosheets. *Procedia Eng.* **32**, 759–764 (2012).
- Qu, H. et al. A review of graphene-oxide/metal-organic framework composites materials: characteristics, preparation and applications. *J. Porous Mater.* **28**, 1837–1865 (2021).
- Navarro, D. A., Kah, M., Losic, D., Kookana, R. S. & McLaughlin, M. J. Mineralisation and release of 14 C-graphene oxide (GO) in soils. *Chemosphere* **238**, 124558 (2020).
- Yin, D. et al. Functional graphene oxide as a plasmid-based Stat3 siRNA carrier inhibits mouse malignant melanoma growth *in vivo*. *Nanotechnology* **24**, 105102 (2013).
- Hu, X. et al. Graphene quantum dots nonmonotonically influence the horizontal transfer of extracellular antibiotic resistance genes via bacterial transformation. *Small* **19**, 2301177 (2023).
- Singh, Y. et al. Nanoparticles as novel elicitors in plant tissue culture applications: current status and future outlook. *Plant Physiol. Biochem.* **203**, 108004 (2023).
- Ge, S. et al. Effects of Graphite oxide on seed germination of solanaceous plants. *J. Shanxi Datong Univ.* **38**, 5–8 (2022).
- Liu, L. & Lu, H. Effects of Graphite oxide on seed germination and seedling growth of *Amorpha fruticosa*. *Seed* **41**, 14–18 + 37 (2022).
- Zhou, Z. et al. Effects of Graphene Oxide on the growth and photosynthesis of the Emergent Plant *Iris pseudacorus*. *Plants* **12**, 1738 (2023).
- Cao, H. et al. Effect of Graphite oxide on wheat seed germination and seedling growth under salt stress. *J. SHANXI Agric. Univ. (Nat. Sci. Ed.)* **42**, 84–92 (2022).
- Zhang, Z. et al. Effects of seed soaking with Graphite oxide on the growth, development and yield of *Brassica napus*. *J. Henan Agricultural Sci.* **52**, 74–80 (2023).
- Zhao, L., Song, R., Wu, Q. & Wu, X. Effect of graphene oxide on seedling growth and physiological characteristics of maize. *JAES* **40**, 1167–1173 (2021).
- Hu, X., Lu, K., Mu, L., Kang, J. & Zhou, Q. Interactions between graphene oxide and plant cells: regulation of cell morphology, uptake, organelle damage, oxidative effects and metabolic disorders. *Carbon* **80**, 665–676 (2014).

21. Chen, J., Wang, X. & Han, H. A new function of graphene oxide emerges: inactivating phytopathogenic bacterium *Xanthomonas oryzae* Pv. *J. Nanopart. Res.* **15**, 1658 (2013).
22. Hu, W. et al. Graphene-based antibacterial paper. *ACS Nano* **4**, 4317–4323 (2010).
23. Liu, S. et al. Antibacterial activity of Graphite, Graphite Oxide, Graphene Oxide, and reduced Graphene Oxide: membrane and oxidative stress. *ACS Nano* **5**, 6971–6980 (2011).
24. Li, S. et al. Efficient gene silencing in Intact Plant cells using siRNA delivered by functional Graphene Oxide nanoparticles. *Angew Chem. Int. Ed.* **61**, e202210014 (2022).
25. Tao, H. et al. Inhibition of algal growth in hydroponic nutrient solution by copper (II)—polyphenol nanocomposite. *China Agric. Univ.* **28**, 106–119 (2023).
26. Dong, W., Wu, D., Wang, C., Liu, Y. & Wu, D. Characterization of the molecular mechanism underlying the dwarfism of dsh mutant watermelon plants. *Plant Sci.* **313**, 111074 (2021).
27. Ren, Y. et al. A tonoplast sugar transporter underlies a sugar accumulation QTL in watermelon. *Plant. Physiol.* **176**, 836–850 (2018).
28. Liu, Y. et al. Transgenic technology for transforming exogenous DNA using pollen tube pathway method. *North. Rice* **44**, 74–77 (2014).
29. Yang, Y. et al. Effects of graphene oxide on plant growth: a review. *Plants* **11**, 2826 (2022).
30. Begum, P. et al. Phytotoxicity of multi-walled carbon nanotubes assessed by selected plant species in the seedling stage. *ASS* **262**, 120–124 (2012).
31. Liu, C. et al. Integrating transcriptome and physiological analyses to elucidate the molecular responses of buckwheat to graphene oxide. *J. Hazard. Mater.* **424**, 127443 (2022).
32. Wang, X. & Chen, J. Research progress on the toxic effects of graphene oxide on algae. *J. Qu Fu Normal Univ.* **48**, 94–99 (2022).
33. Debroy, A. et al. EPS-corona formation on graphene family nanomaterials (GO, rGO and graphene) and its role in mitigating their toxic effects in the marine alga *Chlorella* sp. *Environ. Pollut.* **341**, 123015 (2024).
34. Zhang, Y. et al. In-situ responses of phytoplankton to graphene photocatalysis in the eutrophic lake Xingyun, southwestern China. *Chemosphere* **278**, 130489 (2021).
35. Ahmad, N. S., Abdullah, N. & Yasin, F. M. Toxicity assessment of reduced graphene oxide and titanium dioxide nanomaterials on gram-positive and gram-negative bacteria under normal laboratory lighting condition. *Toxicol. Rep.* **7**, 693–699 (2020).
36. Perreault, F., de Faria, A. F., Nejati, S. & Elimelech, M. Antimicrobial properties of Graphene Oxide nanosheets: why size matters. *ACS Nano* **9**, 7226–7236 (2015).
37. Azarniya, A., Eslahi, N., Mahmoudi, N. & Simchi, A. Effect of graphene oxide nanosheets on the physico-mechanical properties of chitosan/bacterial cellulose nanofibrous composites. *Compos. Part. Appl. Sci. Manuf.* **85**, 113–122 (2016).
38. Butler, A. J., Osborne, L., El Mohtadi, M. & Whitehead, A. Graphene derivatives potentiate the activity of antibiotics against *Enterococcus faecium*, *Klebsiella pneumoniae* and *Escherichia coli*. *AIMS Bioeng.* **7**, 106–113 (2020).
39. Nichols, F. & Chen, S. Graphene Oxide Quantum dot-based functional nanomaterials for effective antimicrobial applications. *Chem. Rec.* **20**, 1505–1515 (2020).
40. Ghorbanpour, M., Farahani, A. & Hadian, J. Potential toxicity of nano-graphene oxide on callus cell of *Plantago major* L. under polyethylene glycol-induced dehydration. *Ecotoxicol. Environ. Saf.* **148**, 910–922 (2018).
41. Li, J. et al. The mutual effects of graphene oxide nanosheets and cadmium on the growth, cadmium uptake and accumulation in rice. *Plant. Physiol. Biochem.* **147**, 289–294 (2020).
42. Ye, W. et al. Calcium decreases cadmium concentration in root but facilitates cadmium translocation from root to shoot in rice. *J. Plant. Growth Regul.* **39**, 422–429 (2020).
43. Hu, X. et al. Effect of graphene on the growth and development of raspberry tissue culture seedlings. *Carbon* **158**, 931 (2020).
44. Qin, H. et al. MicroRNA-29b/graphene oxide–polyethyleneglycol–polyethyleneimine complex incorporated within chitosan hydrogel promotes osteogenesis. *Front. Chem.* **10**, 145 (2022).
45. Saroj, S. et al. Herb extracellular Vesicle-Chitosan-PEGylated graphene oxide conjugate delivers estrogen receptor α targeting siRNA to breast cancer cells. *ACS Appl. Bio Mater.* **7**, 2741–2751 (2024).
46. Takeuchi, H. & Higashiyama, T. Tip-localized receptors control pollen tube growth and LURE sensing in Arabidopsis. *Nature* **531**, 245–248 (2016).
47. Xu, J., Zhang, X., Zhang, Y. & Ma, J. A preliminary study on the introduction of antimicrobial peptide gene Gnk2-1 into watermelon by pollen tube channel method. *Acta Horticult. Sin.* **41**, 1467–1475 (2014).
48. Xu, L. Establishment and optimization of *Agrobacterium tumefaciens*-mediated genetic transformation system in melon. *Chin. Acad. Agricultural Sci.* (2023).
49. Bruna, T., Maldonado-Bravo, F., Jara, P. & Caro, N. Silver nanoparticles and their antibacterial applications. *Int. J. Mol. Sci.* **22**, 7202 (2021).
50. Xu, X. et al. Nanoparticle-dsRNA treatment of Pollen and Root systems of diseased plants effectively reduces the rate of Tobacco Mosaic Virus in Contemporary seeds. *ACS Appl. Mater. Interfaces* **15**, 29052–29063 (2023).
51. Yong, J. et al. Sheet-like clay nanoparticles deliver RNA into developing pollen to efficiently silence a target gene. *Plant. Physiol.* **187**, 886–899 (2021).
52. Tao, Y., Ju, E., Ren, J. & Qu, X. Immunostimulatory oligonucleotides-loaded cationic graphene oxide with photothermally enhanced immunogenicity for photothermal/immune cancer therapy. *Biomaterials* **35**, 9963–9971 (2014).
53. Fávoro, W. J. et al. Hybrid graphene oxide as carrier of doxorubicin: cytotoxicity and preliminary in vivo assays against bladder cancer. *Adv. Nat. Sci: Nanosci. Nanotechnol.* **11**, 025016 (2020).

Acknowledgements

We thank Springer Nature Author Services (<https://secure.authorservices.springernature.com/>) for editing the English text of a draft of this manuscript (Order number H4F8T8RM).

Author contributions

W.D. designed the experiment. Y.Q. and W.D. wrote the main manuscript text. S.H., L. Z., P. N., F. X and D. W. prepared Figs. 1 and 2. Y.Q. prepared Fig. 3. Y.Q. and C.Y. prepared Figs. 4 and 5. All authors reviewed the manuscript.

Funding

This work was supported by funding from the National Natural Science Foundation of China (31801882) and the Henan Province Key Science and Technology Projects (242102111085).

Competing interests

The authors declare no competing interests.

Consent for publication

All authors have approved the manuscript and agree with its submission.

Additional information

Supplementary Information The online version contains supplementary material available at <https://doi.org/10.1038/s41598-025-89361-x>.

Correspondence and requests for materials should be addressed to W.D.

Reprints and permissions information is available at www.nature.com/reprints.

Publisher's note Springer Nature remains neutral with regard to jurisdictional claims in published maps and institutional affiliations.

Open Access This article is licensed under a Creative Commons Attribution-NonCommercial-NoDerivatives 4.0 International License, which permits any non-commercial use, sharing, distribution and reproduction in any medium or format, as long as you give appropriate credit to the original author(s) and the source, provide a link to the Creative Commons licence, and indicate if you modified the licensed material. You do not have permission under this licence to share adapted material derived from this article or parts of it. The images or other third party material in this article are included in the article's Creative Commons licence, unless indicated otherwise in a credit line to the material. If material is not included in the article's Creative Commons licence and your intended use is not permitted by statutory regulation or exceeds the permitted use, you will need to obtain permission directly from the copyright holder. To view a copy of this licence, visit <http://creativecommons.org/licenses/by-nc-nd/4.0/>.

© The Author(s) 2025